THE JOURNAL OF BIOLOGICAL CHEMISTRY VOL. 288, NO. 23, pp. 16680–16689, June 7, 2013

IOP1 Protein Is an External Component of the Human Cytosolic Iron-Sulfur Cluster Assembly (CIA) Machinery and Functions in the MMS19 Protein-dependent CIA Pathway*

Received for publication, December 10, 2012, and in revised form, April 8, 2013 Published, JBC Papers in Press, April 12, 2013, DOI 10.1074/jbc.M112.416602

Mineaki Seki[‡1], **Yukiko Takeda**[‡], **Kazuhiro Iwai**[‡§], **and Kiyoji Tanaka**[‡2]

From the [‡]*Graduate School of Frontier Biosciences, Osaka University, Suita, Osaka 565-0871 and the* [§]*Graduate School of Medicine, Kyoto University, Sakyo-ku, Kyoto 606-8501, Japan*

Background: The CIA machinery in human cells is unclear.
Results: MMS19 formed a complex with MIP18, CIAO1, and IOP1, but IOP1 behaved differently from the other components.
Conclusion: The CIA complex consists of a core MMS19-MIP18-CIAO1 complex, and IOP1 is an external component of the CIA machinery.
Significance: This study increases the understanding of the composition of the CIA machinery in human cells and the interactions between the components.

The emerging link between iron metabolism and genome integrity is increasingly clear. Recent studies have revealed that MMS19 and cytosolic iron-sulfur cluster assembly (CIA) factors form a complex and have central roles in CIA pathway. However, the composition of the CIA complex, particularly the involvement of the Fe-S protein IOP1, is still unclear. The roles of each component are also largely unknown. Here, we show that MMS19, MIP18, and CIAO1 form a tight "core" complex and that IOP1 is an "external" component of this complex. Although IOP1 and the core complex form a complex both *in vivo* and *in vitro*, IOP1 behaves differently *in vivo*. A deficiency in any core component leads to down-regulation of all of the components. In contrast, IOP1 knockdown does not affect the level of any core component. In MMS19-overproducing cells, other core components are also up-regulated, but the protein level of IOP1 remains unchanged. IOP1 behaves like a target protein in the CIA reaction, like other Fe-S helicases, and the core complex may participate in the maturation process of IOP1. Alternatively, the core complex may catch and hold IOP1 when it becomes mature to prevent its degradation. In any case, IOP1 functions in the MMS19-dependent CIA pathway. We also reveal that MMS19 interacts with target proteins. MIP18 has a role to bridge MMS19 and CIAO1. CIAO1 also binds IOP1. Based on our *in vivo* and *in vitro* data, new models of the CIA machinery are proposed.

DNA repair systems have evolved to function in coordination with other cellular metabolic pathways. A genetic framework for studying such coordinated mechanisms in eukaryotic cells was provided by the isolation and phenotypic characterization of mutant strains of the budding yeast *Saccharomyces cerevisiae* that are hypersensitive to DNA-damaging agents (1). The *mms19* mutants were originally isolated in a screening for yeast mutants hypersensitive to the alkylating agent methyl methanesulfonate (MMS).[3] In addition, *mms19* mutants exhibit pleiotropic phenotypes, including methionine auxotrophy, sporulation deficiency, and telomere abnormality (1, 2) and compromised nucleotide excision repair (NER) and temperature-sensitive defects in transcription (3, 4). However, the roles of yeast Mms19 in the maintenance of eukaryotic genome integrity have remained poorly understood. Human MMS19 expressed in yeast can complement the *mms19* phenotypes (5). These phenotypes, which are reminiscent of those resulting from mutations in the basal transcription factor TFIIH, can be corrected *in vitro* by supplementing extracts with TFIIH but not with recombinant yeast Mms19 (3). Human MMS19 directly interacts with the TFIIH components XPD and XPB, which are essential for normal NER (6). Yeast Mms19 itself apparently does not participate directly in NER because it is not required for a reconstituted *in vitro* NER system (7), but recent studies by Kou *et al.* show that yeast Mms19 functions indirectly in NER by maintaining an adequate cellular concentration of the TFIIH subunit Rad3, a yeast counterpart of human XPD. However, the temperature-sensitive growth defect of *mms19* is not rescued by artificially maintaining an adequate amount of Rad3, indicating that yeast Mms19 serves as a multifunctional regulator in the maintenance of genome integrity (8).

Fe-S clusters are ancient versatile protein cofactors involved in multiple fundamental processes, including electron transfer, enzyme catalysis, and gene expression (9, 10). Fe-S clusters are used for transferring electrons, generating radicals, and stabilizing protein structures. An Fe-S cluster is involved in DNA damage recognition by the *Escherichia coli* MutY protein,

* This work was supported by Grant-in-aid for Scientific Research (C) 22510061 (to M. S.) and a Grant-in-aid for Scientific Research on Innovative Areas (to K. T.) from the Ministry of Education, Culture, Sports, Science, and Technology of Japan (MEXT) and by Health and Labor Sciences Research Grants for Research on Intractable Diseases (to K. T.).
[1] To whom correspondence may be addressed. E-mail: mseki@fbs.osaka-u.ac.jp.
[2] To whom correspondence may be addressed. E-mail: ktanaka@fbs.osaka-u.ac.jp.

[3] The abbreviations used are: MMS, methyl methanesulfonate; NER, nucleotide excision repair; TF, transcription factor; CIA, cytosolic iron-sulfur cluster assembly; MMC, mitomycin C.

which functions in oxidative DNA damage repair (11). Several nuclear helicases belonging to the XPD/Rad3 family contain Fe-S clusters (12, 13). The crystal structure of one of these, XPD from archaea, revealed that the Fe-S cluster plays a role in maintaining the structure of XPD helicases (14–16). The domain of XPD containing the Fe-S cluster has a wedge-like feature that is involved in DNA duplex separation during unwinding (13, 16).

Previously, we reported that human MMS19 and XPD form a novel TFIIH-independent protein complex, which we named MMXD, consisting of MMS19, XPD, MIP18, ANT2, and CIAO1 (17). CIAO1 is involved in the late step of cytosolic iron-sulfur cluster assembly (CIA) (18). Recently, MMS19 was reported to form a complex with the CIA machinery. Here, we describe the composition of the complex, the interactions between the components in the complex, and the roles of each component.

EXPERIMENTAL PROCEDURES

Cell Culture—The HeLa, MCF7, and HEK293 cell lines were used in this study. Each cell line was cultured in DMEM containing 10% fetal bovine serum and 100 units/ml penicillin/streptomycin at 37 °C in a 5% CO_2 incubator.

Isolation of Stable Transfectants—HEK293 cells overexpressing FLAG-His_6-MMS19 were transfected with a pcDNA3 vector containing human HA-CIAO1. Stable transfectants were selected in the presence of G418.

Plasmids—A vector-based RNAi approach (shRNA) was used to knock down MMS19 in HeLa cells. A gene-specific targeting sequence (shMMS19-KD1, GGATGAATTCCTACAGCTA) was cloned into the pSUPERIOR vector (Oligoengine) to obtain vector-encoded short hairpin constructs for RNAi. Another gene-specific targeting sequence (shMMS19-KD2, TGATGGCTTCTCTCTGCTCATGTCTGACT) and the expression vector pRS were purchased from OriGene.

Purification of Protein Complexes—The FLAG-His_6-MMS19 complex was purified from HEK293 cells overexpressing FLAG-His_6-MMS19 as described previously (17). The complex between FLAG-His_6-MMS19 and HA-CIAO1 was purified by sequential affinity purification with anti-FLAG M2-agarose (Sigma-Aldrich), followed by anti-HA agarose (Sigma-Aldrich), as described previously (19).

Protein-Protein Interaction Assay—The recombinant proteins (1 pmol each) were incubated in NETN buffer (17) containing 100 μg/ml BSA for 3–4 h and pulled down with the appropriate affinity tag resins. After several washes, bound proteins were eluted and analyzed by immunoblot analysis.

Gel Filtration—Sf9 cell extracts overexpressing FLAG-His_6-MMS19, His-CIAO1, His-MIP18, and His-IOP1 were mixed and incubated for 3 h to form a complex. The MMS19 complex was then isolated by FLAG tag affinity purification and subjected to Superose 6 PC 3.2/30 (GE Healthcare) with buffer containing 20 mM Tris-HCl (pH 8.0), 150 mM NaCl, 10% glycerol, 0.1% Tween 20, and 10 mM 2-mercaptoethanol.

Cell Survival Assays—Cells were plated in 10-cm dishes at a density of 1000–2000 cells/dish. After 24 h, cells were washed with PBS and irradiated with γ-rays at the indicated doses. For mitomycin C (MMC) and MMS treatment, cells were incubated with the indicated amount of the agent for 1 h. Cells were then washed with PBS and incubated for 1–2 weeks. The resulting colonies were fixed with 3.7% formaldehyde, stained with 0.1% crystal violet, and counted using a binocular microscope.

Subcellular Fractionation—Cells were fractionated into the cytosol (fraction 1), membranes and organelles (fraction 2), nucleus (fraction 3), and cytoskeleton (fraction 4) using selected buffers from the Merck subcellular proteome extraction kit.

FANCD2 Monoubiquitylation Analysis—Cells were treated with 0.5 μM MMC for 1 h to induce FANCD2 monoubiquitylation.

Knockdown Experiments—The siRNA duplexes used in this study are listed below. siRNA duplexes specifically targeting *MMS19*, *CIAO1*, and *IOP1* (Stealth RNA) and non-targeting control siRNAs were purchased from Invitrogen. All siRNAs were transfected using Lipofectamine RNAiMAX (Invitrogen). The sequences of the siRNAs were as follows: *CIAO1*, AGUGGUUACACACUCAAAGUCAUCC; *MMS19*, UACGGAUGCCAACAAGCUGAAGCUG; and *IOP1*, AGCACGUGGAGAGACUGUACGGCAU. siRNA duplexes specifically targeting *MIP18* and *XPD* (SMARTpool) were purchased from Dharmacon and were as described previously (17). Knockdown efficiencies were verified by immunoblotting or real-time quantitative PCR using TaqMan probes (Applied Biosystems).

Western Blotting and Antibodies—Antibodies against MMS19, MIP18, and XPD were described previously (17). Polyclonal antibody against human CIAO1 was raised in rabbits. Other antibodies were purchased commercially: anti-FANCJ, anti-GAPDH, and anti-actin (Sigma-Aldrich); anti-RTEL1 (D-20) and anti-POLE (Santa Cruz Biotechnology); anti-IOP1 (Abcam); anti-MLH1 (BD Pharmingen); anti-NUBP1 (Abnova); anti-RTEL1 (LifeSpan); anti-FANCD2 (Novus); and anti-PRIM2 (Cell Signaling). For some Western blot experiments, a rapid Western blot apparatus (Western Q, SciTrove) was used.

RESULTS

Knockdown of MMS19 Results in Hypersensitivity to Killing by MMC in HeLa Cells—Previously, we showed that MMS19-knockdown HeLa cells are sensitive to UV light (17). To study the roles of MMS19 in DNA repair pathways further, we generated two independent shRNA-mediated MMS19-knockdown HeLa cell lines (shMMS19-KD clones 1 and 2) and measured their sensitivity to a range of DNA-damaging agents. Both clones behaved qualitatively similarly in all of the experiments described below. Compared with HeLa cells, shMMS19-KD cells exhibited hypersensitivity to the cross-linking agent MMC and moderate sensitivity to γ-rays and MMS (Fig. 1, *C–E*).

Protein Levels of FANCJ and RTEL1 Are Reduced in MMS19-knockdown Cells—The Fanconi anemia pathway is essential for repair of DNA interstrand cross-links. Central to the Fanconi anemia pathway is the monoubiquitylation of FANCD2 (20). We found that FANCD2 was monoubiquitylated normally in MMS19-knockdown HeLa cells (Fig. 2*D*). Therefore, we focused on proteins that act downstream of FANCD2 in the DNA cross-link repair pathway. One such protein is FANCJ, a member of the XPD/Rad3 Fe-S helicase family (21). The level of XPD is reduced in MMS19-knockdown cells (17), prompting us to investigate the level of FANCJ in these cells. As shown in Fig.

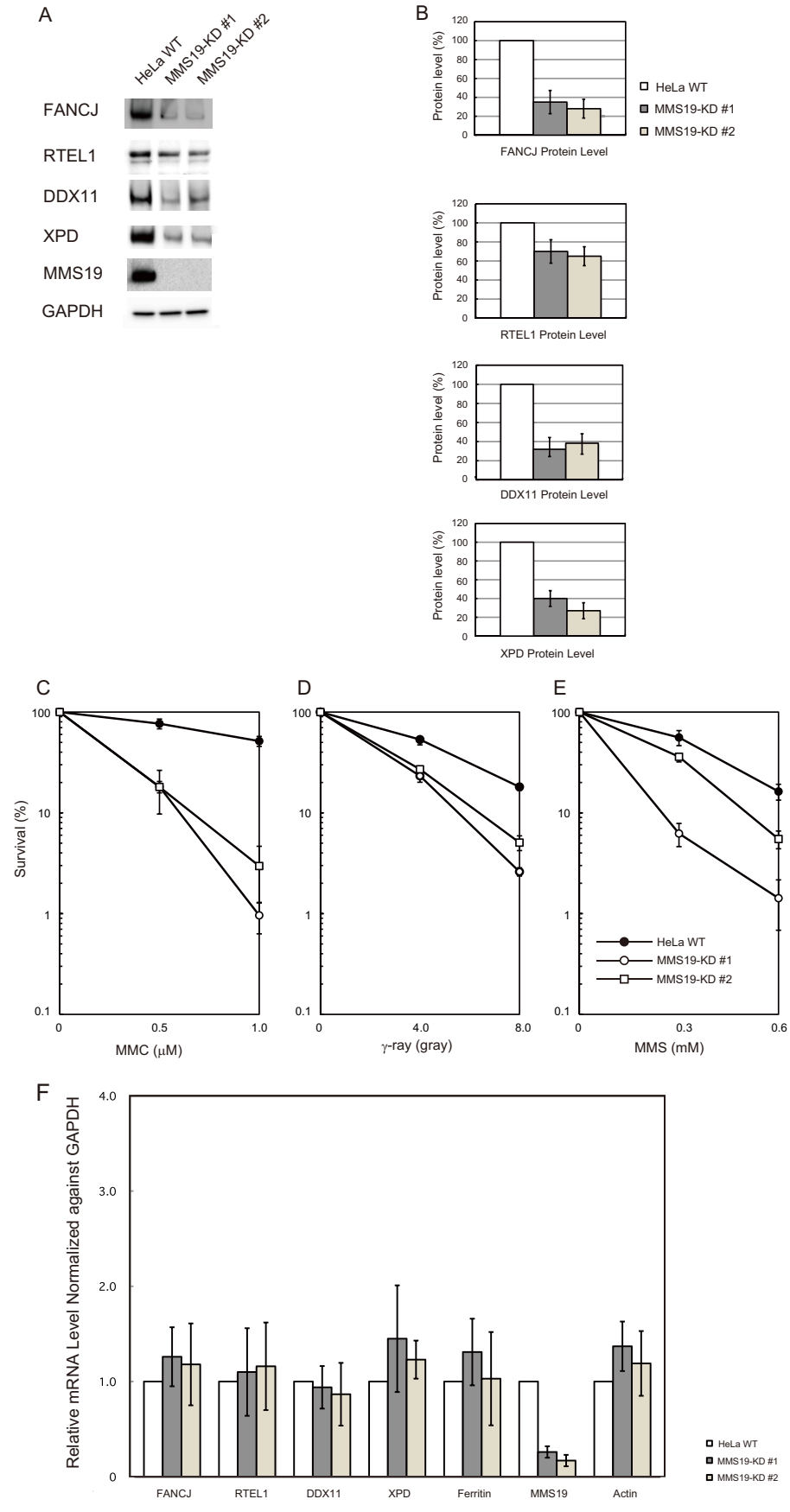
A
HeLa WT
MMS19-KD #1
MMS19-KD #2
FANCJ
RTEL1
DDX11
XPD
MMS19
GAPDH
B
Protein level (%)
FANCJ Protein Level
RTEL1 Protein Level
DDX11 Protein Level
XPD Protein Level
HeLa WT
MMS19-KD #1
MMS19-KD #2
C
D
E
Survival (%)
MMC (μM)
γ-ray (gray)
MMS (mM)
F
Relative mRNA Level Normalized against GAPDH
FANCJ
RTEL1
DDX11
XPD
Ferritin
MMS19
Actin

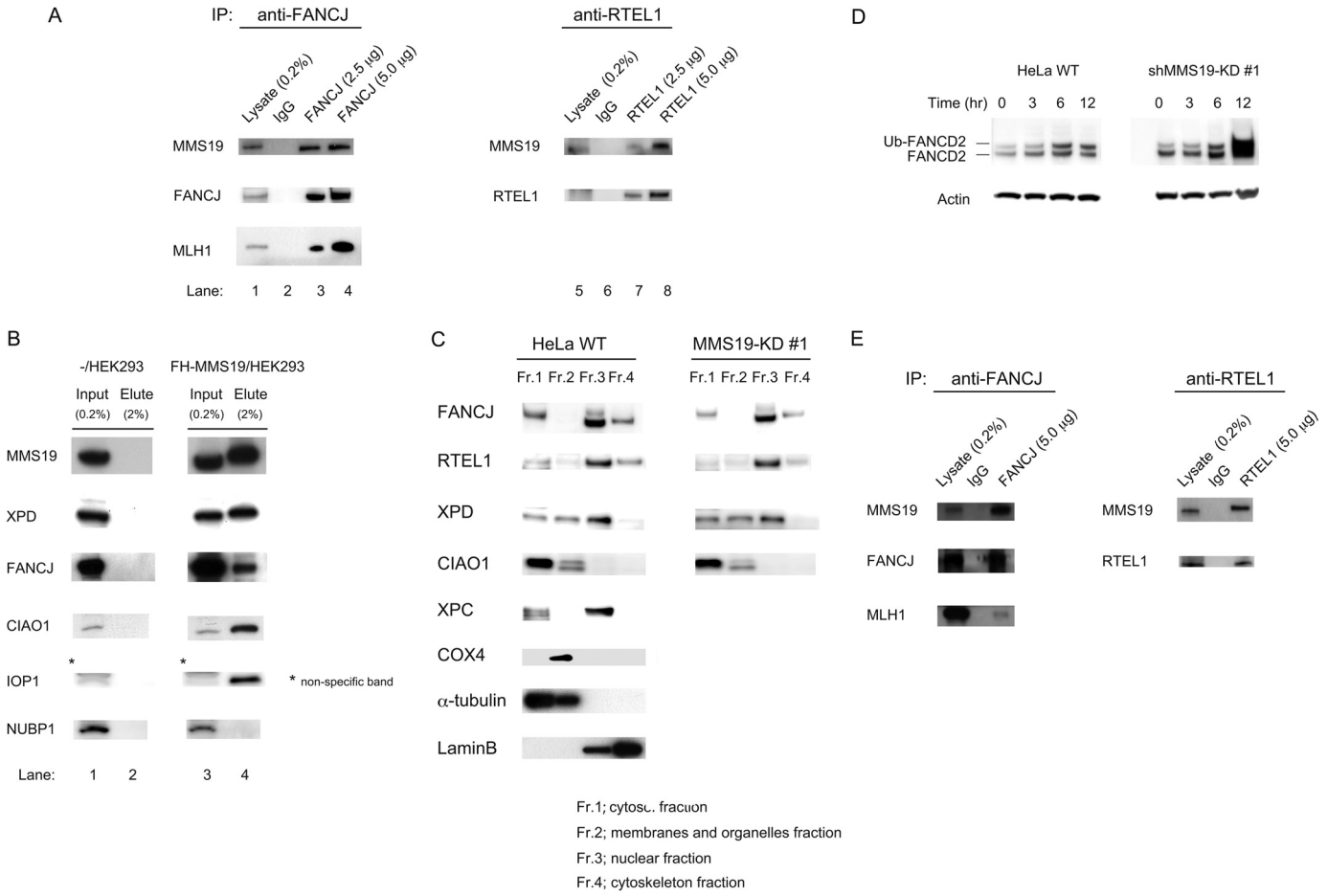

FIGURE 2. **MMS19 interacts with Fe-S helicases *in vivo*.** *A*, MCF7 whole-cell extracts (lysates) were incubated with either rabbit anti-FANCJ or anti-RTEL1 polyclonal antibody. Immunoprecipitates (*IP*) were analyzed using antibodies against the indicated proteins. *B*, a whole-cell extract from HEK293 cells overexpressing FLAG-His-MMS19 (*FH-MMS19/HEK293*) and the purified FLAG-His$_6$-MMS19 complex isolated from the whole-cell extract were immunoblotted with antibodies against the indicated proteins. HEK293 whole-cell extract (*−/HEK293*) was used as a control. *C*, MMS19 knockdown does not affect the subcellular localization of Fe-S helicases. Subcellular localization was examined by immunoblot analysis using the indicated antibodies. Subcellular fractionations of Fe-S helicases were in wild-type HeLa and shMMS19-KD (clone 1; *MMS19-KD #1*) cells. Whole cell extracts were separated into fractions as described under "Experimental Procedures." Protein markers for the fractions are as follows: fraction (*Fr.*) 1, α-tubulin; fraction 2, COX4; fraction 3, XPC; and fraction 4, laminB. *D*, damage-induced FANCD2 monoubiquitylation is unaffected by MMS19 knockdown. Whole-cell extracts were incubated with anti-FANCD2 antibody. FANCD2 monoubiquitylation (*Ub-FANCD2*) was induced as described under "Experimental Procedures." FANCD2 monoubiquitylation was ascertained by slower electrophoretic migration. Actin was used as a loading control. *E*, MMS19 interacts with Fe-S helicases *in vivo*. HeLa whole-cell extracts (lysates) were incubated with either rabbit anti-FANCJ or anti-RTEL1 polyclonal antibody. Immunoprecipitates were analyzed using antibodies against the indicated proteins.

1 (*A* and *B*), the levels of FANCJ were markedly reduced in shMMS19-KD cells compared with WT cells. RTEL1, another member of the XPD/Rad3 Fe-S helicase family, is required for telomere maintenance and homologous recombination (22); the levels of RTEL1 were also decreased in shMMS19-KD cells (Fig. 1, *A* and *B*). DDX11 is another member of the Fe-S cluster-containing DNA helicase family, and it is involved in sister chromatid cohesion and unwinding of the intermediates of DNA replication and recombination. As with the other helicases, the levels of DDX11 were significantly decreased in shMMS19-KD cells (Fig. 1, *A* and *B*). Studies in yeast suggest that MMS19 deficiency affects the general transcription level in human cells (3, 8). Thus, we examined the mRNA levels of Fe-S helicases in MMS19-deficient cells. No relative reduction compared with the control mRNA level was observed (Fig. 1*F*).

Interaction of MMS19 with Fe-S Helicases in Human Whole-cell Extracts—We investigated whether MMS19 interacts directly with FANCJ or RTEL1. To this end, we performed immunoprecipitation experiments using whole-cell extracts derived from MCF7 breast cancer cells. Anti-FANCJ antibody precipitated MMS19 from whole-cell extracts (Fig. 2*A*, *lanes 3* and *4*), whereas neither FANCJ nor MMS19 was precipitated

FIGURE 1. **Protein levels of nuclear Fe-S helicases are reduced in HeLa cells following knockdown of MMS19.** *A*, immunoblots of whole-cell extracts using the indicated antibodies. Data shown are from one of several representative experiments. GAPDH was used a loading control. *MMS19-KD #1* and *MMS19-KD #2*, shMMS19-KD clones 1 and 2, respectively. *B*, histograms show mean protein levels of Fe-S helicases. *Error bars* indicate S.D. calculated from at least three independent experiments in WT and shMMS19-KD (clones 1 and 2) cells. *C–E*, WT and shMMS19-KD (clones 1 and 2) cells were treated with the indicated amounts of MMC (*C*), γ-rays (*D*), and MMS (*E*). Each *data points* represent mean values of at least three independent experiments; *error bars* indicate the S.D. *F*, real-time quantitative PCR analyses were performed with cDNAs prepared from WT and shMMS19-KD (clones 1 and 2) cells. Histograms represent the mean values of the indicated mRNAs, normalized against GAPDH mRNA. *Error bars* indicate S.D. calculated from three independent experiments.

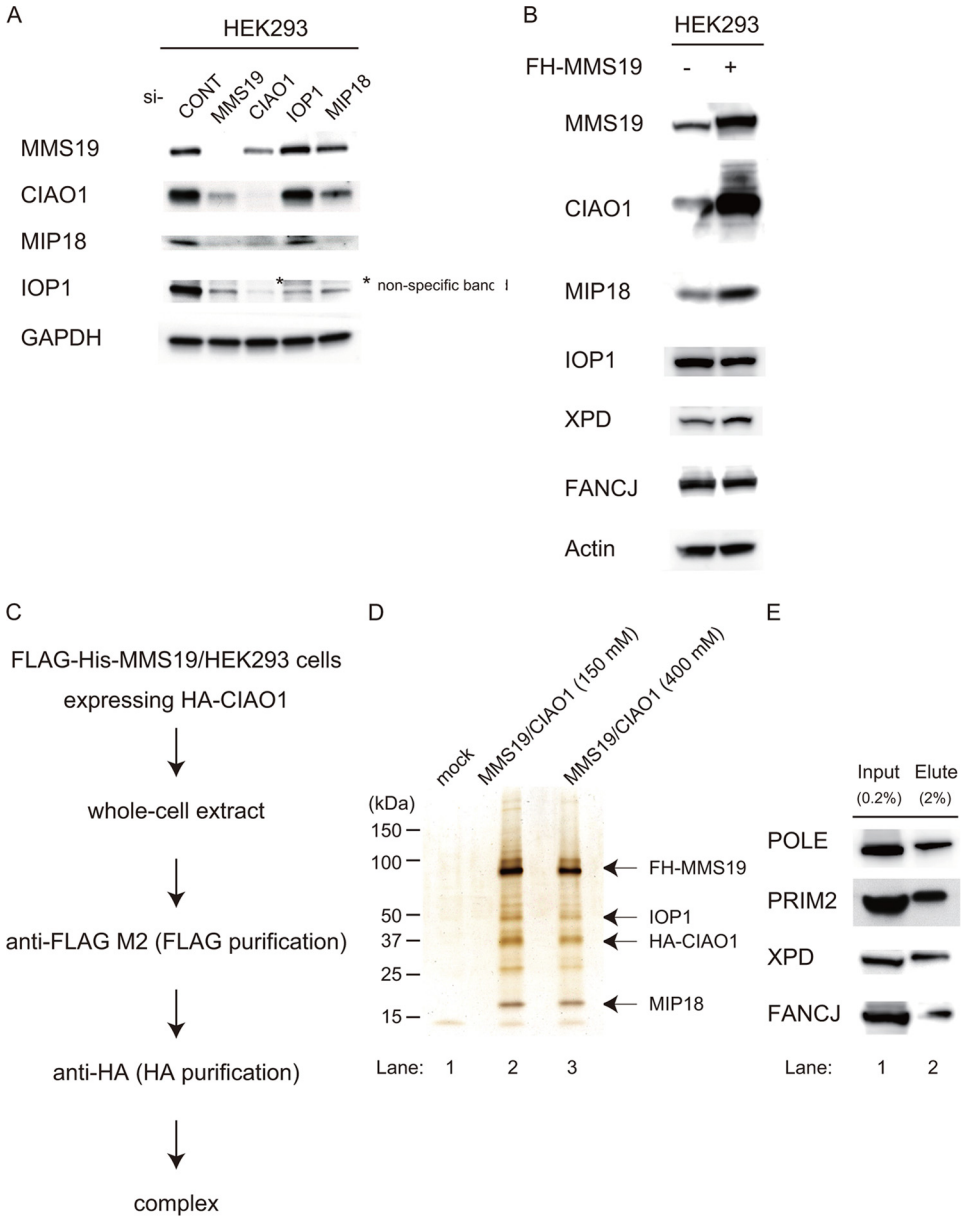

FIGURE 3. **MMS19 knockdown down-regulates CIA machinery.** *A*, immunoblots of whole-cell extracts (using the indicated antibodies) from HEK293 cells transfected with control siRNA (*siCONT*) or siRNA specifically targeting *MMS19*, *CIAO1*, *MIP18*, or *IOP1*. *B*, immunoblots of whole-cell extracts (using the indicated antibodies) from wild-type HEK293 cells and HEK293 cells overexpressing FLAG-His$_6$-MMS19 (*FH-MMS19*). *C*, experimental procedure for purification of complexes between FLAG-His$_6$-MMS19 and HA-CIAO1. *D*, silver staining of the complex between FLAG-His$_6$-MMS19 and HA-CIAO1 purified from HEK293 cells overexpressing both FLAG-His$_6$-MMS19 and HA-CIAO1 in normal salt (150 mM NaCl; *lane 2*) and high salt (400 mM NaCl; *lane 3*). As a control, a mock purification was performed with whole-cell extract prepared from non-transfected HEK293 cells (*lane 1*). *E*, whole-cell extracts from HEK293 cells overexpressing FLAG-His$_6$-MMS19 and HA-CIAO1 were immunoblotted with antibodies against the indicated proteins (*lane 1*). The purified complex between FLAG-His$_6$-MMS19 and HA-CIAO1 isolated from the whole-cell extracts was immunoblotted with antibodies against the indicated proteins (*lane 2*).

when normal rabbit IgG was used (*lane 2*). In control experiments, MLH1, a known binding partner of FANCJ (23), was co-immunoprecipitated with anti-FANCJ antibody. MMS19 was also co-immunoprecipitated with anti-RTEL1 antibody in a manner dependent on antibody concentration (Fig. 2*A*, *lanes 7* and *8*). Similar effects were observed in HeLa cells (Fig. 2*E*).

Next, we expressed FLAG-His$_6$-MMS19 protein in HEK293 cells and performed affinity purification of whole-cell extracts (17). Immunoblots revealed that the FLAG-His$_6$-MMS19 complex contained FANCJ, XPD, and CIAO1 (Fig. 2*B*, *lane 4*). The yeast ortholog of CIAO1, Cia1, interacts with Nar1 (18, 24). Nar1 is the yeast ortholog of human IOP1 and is also known as a CIA factor. Consistent with those observations, we also identified human IOP1 in the FLAG-His$_6$-MMS19 complex (Fig. 2*B*). In contrast, we did not detect the NUBP1-NUBP2 complex (Fig. 2*B*), which functions at an earlier stage in CIA pathway (25).

XPD, FANCJ, and RTEL1 normally function in the nucleus, so we examined the subcellular localization of these helicases in shMMS19-KD cells (clone 1). FANCJ, RTEL1, and XPD proteins were present predominantly in the nuclear fraction in both shMMS19-KD and WT cells (Fig. 2*C*). Thus, MMS19 does not affect the nuclear localization of Fe-S helicases.

Isolation of the MMS19-CIAO1 Protein Complex—In MMS19-knockdown HEK293 cells, the protein levels of CIAO1, MIP18,

and IOP1 were markedly decreased (Fig. 3*A*). A similar decrease in protein levels was observed when CIAO1 and MIP18 were knocked down. In contrast, the protein levels of MMS19, MIP18, and CIAO1 were not affected by the knockdown of IOP1 (Fig. 3*A*). Next, we examined the protein levels of CIAO1, MIP18, and IOP1 in HEK293 cells overexpressing FLAG-His_6-MMS19. The protein levels of CIAO1 and MIP18 were markedly elevated in these cells (Fig. 3*B*), whereas the levels of IOP1, XPD, and FANCJ were unchanged (Fig. 3*B*). These results suggest that MMS19 forms a stable complex with CIAO1, MIP18, and IOP1, although IOP1 behaves somewhat differently.

To further analyze the roles of MMS19 and other proteins in CIA, we isolated MMS19 and CIAO1 as a complex from HEK293 cells overexpressing both FLAG-His_6-MMS19 and HA-CIAO1 by affinity purification using anti-FLAG and anti-HA antibodies (Fig. 3, *C* and *D*). Mass spectrometry analysis indicated that the MMS19-CIAO1 complex contains IOP1 and MIP18 (Fig. 3*D*). The MMS19-CIAO1 complex was stable even under high salt concentrations (Fig. 3*D*, *lane 3*). We also tested whether Fe-S helicases and other Fe-S proteins in the nucleus interact with this complex. XPD and FANCJ, as well as two other Fe-S proteins working in DNA replication called POLE and PRIM2, were also identified (Fig. 3*E*).

To further elucidate the complex composition and the roles of each component, all factors were independently purified from extracts of Sf9 cells overexpressing each protein (Fig. 4*A*). The complex composition was examined by gel filtration analysis, and a complex consisting of all the four proteins (MMS19, MIP18, CIAO1, and IOP1) was predominantly formed (Fig. 4*B*). These results provide further support for the idea that MMS19 forms a complex with CIAO1, MIP18, and IOP1.

Next, we investigated direct interactions within the complex by examining pairwise interactions between purified components. FLAG-His_6-MMS19 interacted with His_6-MIP18, as reported previously (17). We observed a weak interaction between FLAG-His_6-MMS19 and His_6-IOP1 (Fig. 4*C*), but no interaction between FLAG-His_6-MMS19 and His_6-CIAO1. When His_6-HA-CIAO1 was used as the bait instead of FLAG-His_6-MMS19, we observed a strong interaction between His_6-HA-CIAO1 and His_6-MIP18 (Fig. 4*D*). His_6-IOP1 interacted with His_6-HA-CIAO1 weakly, and we observed no interaction between His_6-HA-CIAO1 and FLAG-His_6-MMS19. To examine the interaction of the target proteins with the MMS19 complex components, we used FLAG-V5-His_6-XPD and His_6-FANCJ-HA as baits. As reported previously (16), FLAG-V5-His_6-XPD interacted with FLAG-His_6-MMS19 and His_6-MIP18 (Fig. 4*E*). We observed a strong interaction between FLAG-V5-His_6-XPD and His_6-CIAO1. Next, we used another Fe-S helicase, FANCJ, as a bait. His_6-FANCJ-HA interacted with FLAG-His_6-MMS19, but an interaction between His_6-FANCJ-HA and His_6-CIAO1 was not observed (Fig. 4*F*).

DISCUSSION

In this study, we found that MMS19-knockdown cells are hypersensitive to MMC and moderately sensitive to γ-rays and MMS (Fig. 1, *C*–*E*), in addition to the UV sensitivity and abnormal chromosome segregation we reported previously (17). The protein levels of the Fe-S cluster-containing DNA helicase family members FANCJ, RTEL1, DDX11, and XPD are decreased in MMS19-knockdown cells. MMS19 forms a complex with MIP18, CIAO1, and IOP1, and this complex contributes to the CIA machinery. These results suggest that the pleiotropic phenotypes of MMS19-knockdown cells might be explained by decreased levels of the Fe-S proteins due to a defect in CIA.

Pleiotropic Phenotypes in MMS19-knockdown Cells—The levels of the XPD/Rad3 Fe-S helicase family members FANCJ, XPD, DDX11, and RTEL1 were decreased in MMS19-knockdown cells (Fig. 1*B*). FANCJ and RTEL1 are required for DNA cross-link repair; thus, the decreased levels of these proteins may explain the hypersensitivity of MMS19-knockdown cells to MMC (22, 26–28). XPD is a subunit of TFIIH required for NER and basal transcription; decreased levels of XPD result in UV sensitivity and abnormal transcription (29). Deficiency of DDX11, which functions in cohesion, causes impaired chromosome segregation (30). We showed previously that abnormal chromosome segregation is frequently observed in MIP18- and MMS19-knockdown cells (17). Dysfunction of DDX11 caused by impaired Fe-S cluster assembly may explain the frequent abnormal chromosome segregation in MIP18- and MMS19-knockdown cells (17). In addition, a recent study by Netz *et al.* (31) showed that eukaryotic DNA polymerases α, δ, ϵ, and ζ possess Fe-S clusters. Dysfunction in Fe-S DNA polymerases affects cellular sensitivity to multiple DNA-damaging agents (32). We also showed that POLE, a catalytic subunit of DNA polymerase ϵ, and PRIM2, a subunit of primase, interact with MMS19 (Fig. 3*E*). These results suggest that the pleiotropic phenotypes of MMS19-knockdown cells, such as abnormal DNA repair, transcription, and chromosome segregation (3, 17), could be explained by a decrease in the levels of Fe-S proteins. During the preparation of our manuscript, two other groups reported that MMS19 deficiency results in hypersensitivity to some DNA-damaging agents and that MMS19 is involved in the CIA pathway (33, 34). Collectively, the pleiotropic phenotypes of MMS19-knockdown cells are likely caused by a decrease in the levels of Fe-S proteins resulting from a defect in CIA activity. However, the number of Fe-S proteins involved in the maintenance of genome integrity is continually increasing. As described above, general transcription is also affected in MMS19-deficient cells. Thus, the impact of MMS19 deficiency on genome integrity may not be limited to Fe-S proteins involved in DNA metabolism, but may also affect the intracellular environment, potentially resulting in dysregulation of the cellular network that controls genome integrity. Hence, the effects of MMS19 knockdown and impaired CIA activity on genome integrity should be further explored within the context of MMS19 involvement in cell homeostasis.

Roles of Core Components of the MMS19 Complex in CIA—To further elucidate the roles of MMS19 and CIA components in CIA, we examined the interactions between purified recombinant proteins. Previously, we showed that recombinant MMS19 strongly interacts with *in vitro* translated XPD (17). MMS19 also binds two recombinant human Fe-S proteins, XPD and FANCJ (Fig. 4, *E* and *F*). MMS19 contains HEAT repeats that have a rod-shaped structure and often function in

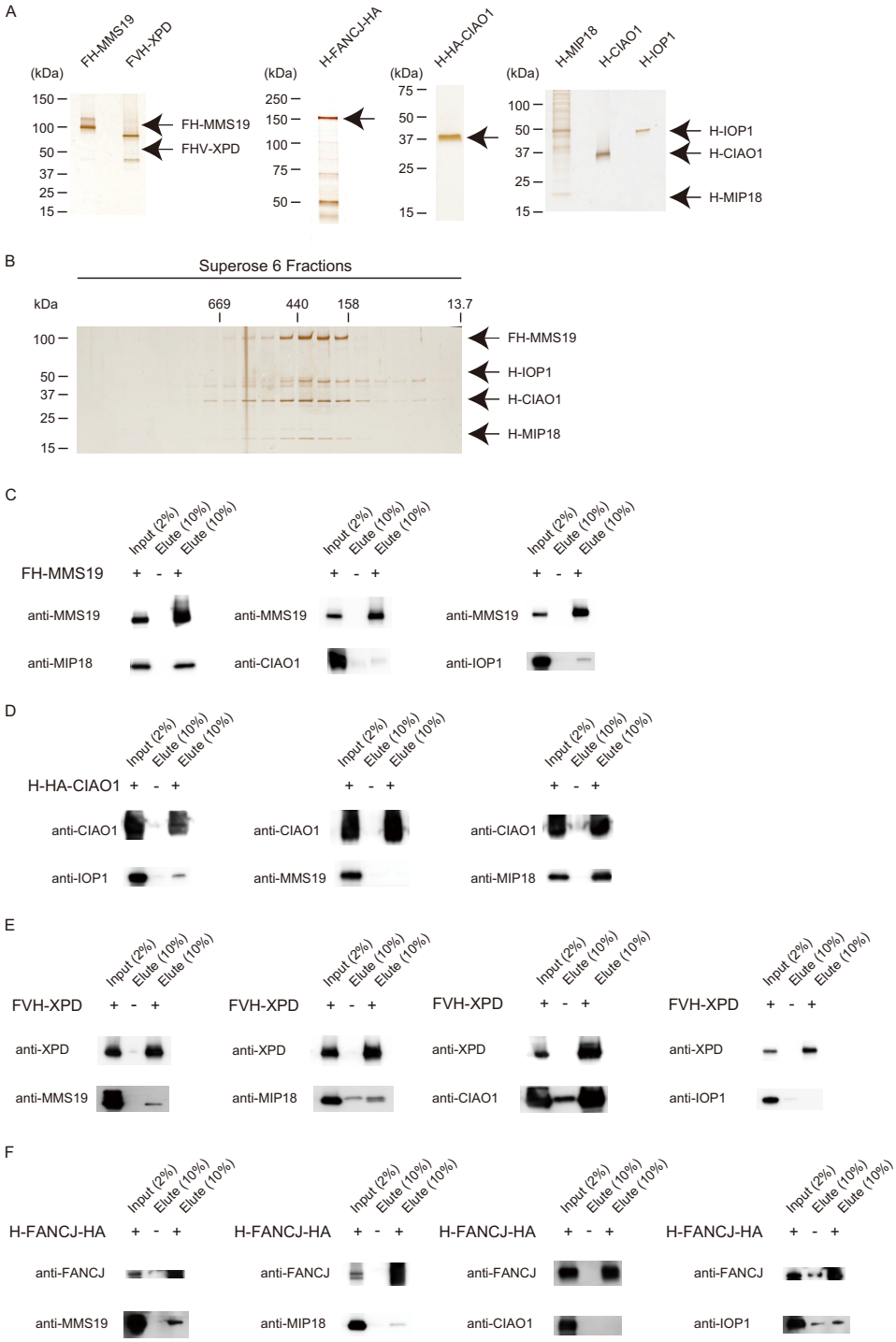

FIGURE 4. **Interactions between MMS19 complex components and target proteins.** *A*, silver staining of recombinant FLAG-His$_6$-MMS19 (*FH-MMS19*), FLAG-V5-His$_6$-XPD (*FVH-XPD*), His$_6$-FANCJ-HA (*H-FANCJ-HA*), His$_6$-HA-CIAO1 (*H-Ha-CIAO1*), His$_6$-MIP18 (*H-MIP18*), His$_6$-CIAO1 (*H-CIAO1*), and His$_6$-IOP1 (*H-IOP1*) proteins purified from insect cells infected with baculoviruses expressing each of these proteins. FLAG-His$_6$-MMS19 and FLAG-V5-His-XPD were affinity-purified using the FLAG tag. His$_6$-FANCJ-HA and His$_6$-HA-CIAO1 were affinity-purified using the HA tag, and other proteins were affinity-purified using the His tag. *B*, the MMS19 complex was separated on a Superose 6 column. After fractionation, each fraction was resolved by SDS-PAGE and visualized by silver staining. *C*, purified FLAG-His$_6$-MMS19 was incubated with the indicated proteins and affinity-captured with FLAG beads. As a control, FLAG-His$_6$-MMS19 was omitted. After repeated washes with NETN buffer, FLAG tag-bound proteins were eluted with FLAG peptide and subjected to immunoblot analysis. *D*, purified His$_6$-HA-CIAO1 was incubated with the indicated proteins and affinity-captured with HA beads. As a control, His$_6$-HA-CIAO1 was omitted. After repeated washes with NETN buffer, HA tag-bound proteins were eluted with HA peptide and subjected to immunoblot analysis. *E*, purified FLAG-V5-His$_6$-XPD was incubated with the indicated proteins and affinity-captured with V5 beads. As a control, FLAG-V5-His$_6$-XPD was omitted. After repeated washes with NETN buffer, V5 tag-bound proteins were subjected to immunoblot analysis. *F*, purified His$_6$-FANCJ-HA was incubated with the indicated proteins and affinity-captured with HA beads. As a control, His$_6$-FANCJ-HA was omitted. After repeated washes with NETN buffer, HA tag-bound proteins were eluted with HA peptide and subjected to immunoblot analysis.

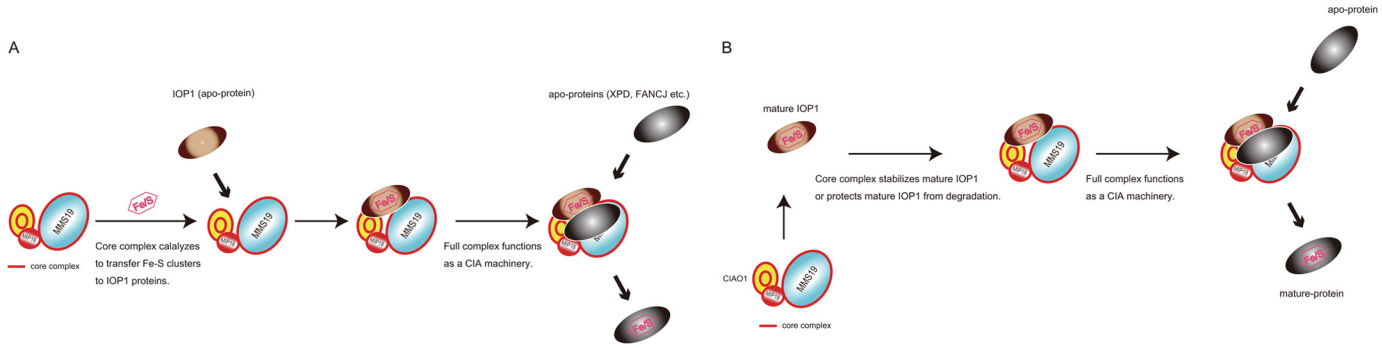

FIGURE 5. **Models for the human CIA machinery.** The MMS19 complex consists of a core complex (MMS19-MIP18-CIAO1) and an external component (IOP1). The core complex catches and holds IOP1 via interaction with CIAO1. MMS19 in the core complex binds apoproteins. MIP18 connects CIAO1 and MMS19. *A*, the core complex (MMS19-MIP18-CIAO1) participates in transferring Fe-S clusters to IOP1 apoproteins. Then, the full complex further catalyzes the Fe-S cluster transfer reaction to the target proteins. *B*, the core complex catches and holds IOP1 when it is matured in the early phase of the CIA pathway. The core complex stabilizes IOP1 or protects IOP1 from degradation. Then, the full complex catalyzes the Fe-S cluster transfer reaction to the target proteins. In either case, IOP1 functions via the MMS19-dependent pathway.

protein transport in the cytosol (35). These results suggest that MMS19 might function in the transport of target proteins. Other core components might participate in the interactions with the target proteins in some cases, just like XPD (Fig. 4*E*) (17). In contrast, our data clearly show that CIAO1 does not interact with FANCJ, and it should be further explored (Fig. 4*F*). CIAO1 is a WD40 protein and may work as a docking base for proteins. In yeast, Cia1 and Nar1 interact with each other (18). Consistent with this, purified CIAO1 interacts with IOP1 (Fig. 4*D*). Moreover, CIAO1 binds tightly to MIP18 (Fig. 4*D*), and MIP18 binds tightly to MMS19 (Fig. 4*C*). Hence, MIP18 plays a role in connecting MMS19 and CIAO1.

The status and roles of IOP1 in the MMS19 complex remain unsolved. IOP1 may function in both the MMS19-dependent and MMS19-independent CIA pathways (34). Alternatively, IOP1 may be included in the MMS19 complex and involved solely in the MMS19 complex-dependent CIA pathway (33). Our immunoprecipitation experiments indicate that CIAO1, MIP18, and IOP1 are present in the MMS19 complex (Fig. 2*B*). Gel filtration data also indicate that IOP1 is likely to present in the MMS19 complex in human cells (Fig. 4*B*). The core components (MMS19, CIAO1, and MIP18) are highly dependent on each other; when one is depleted by siRNA knockdown, other components are down-regulated (Fig. 3*A*). Furthermore, the protein levels of MIP18 and CIAO1 are increased in MMS19-overexpressing cells (Fig. 3*B*). These observations suggest that the core components are tightly associated with each other and become more vulnerable to degradation when they are not incorporated within the complex. In contrast, IOP1 behaves differently; it is down-regulated when one of the core components is depleted, but knockdown of IOP1 does not affect the levels of the core components (Fig. 3*A*). Moreover, the levels of IOP1 remain constant after MMS19 overproduction, as do the levels of the Fe-S helicases XPD and FANCJ (Fig. 3*B*). Considering that Nar1, the yeast IOP1 ortholog, is known to contain multiple Fe-S clusters (24), the MMS19 core complex might participate in IOP1 maturation, and the loss of the core complex might reduce the protein level of IOP1, just like other Fe-S proteins (Fig. 5*A*). Alternatively, the core complex may catch and hold IOP1 immediately after IOP1 is matured in the early phase of the CIA pathway. The core complex may stabilize mature IOP1 or protect mature IOP1 from degradation (Fig. 5*B*). In any case, it is likely that IOP1 functions via the MMS19-dependent pathway in human cells. In contrast, yeast studies show that Mms19 is not essential and that Nar1 is essential in yeast cells, suggesting that Nar1 has more important roles in the CIA pathway compared with Mms19. However, recent studies using knock-out mice have shown that both IOP1 and MMS19 are essential in higher eukaryotes (33, 36, 37). The role of IOP1 and MMS19 in the vertebrate CIA machinery may be different from that of yeast orthologs.

Another model of the MMS19 complex was proposed by van Wietmarschen *al.* during the course of our manuscript preparation (38). They analyzed the protein-protein interactions between CIA components by using *in vitro* translated proteins and have shown a different model. There are several differences between our model and theirs. One major difference is, again, the status of IOP1. According to their model, IOP1 forms a complex with CIAO1, as in the case of yeast orthologs. In contrast, our siRNA-knockdown analyses indicate that CIAO1 instead forms a tight complex with MMS19 and MIP18, but not with IOP1. The roles of MIP18 and CIAO1 are also different. Their experiments indicate that there is no interaction between MMS19 and MIP18. Here, we have shown that recombinant MIP18 produced by insect cells clearly binds MMS19 (Fig. 4*C*). Interaction between MMS19 and CIAO1 was also shown by van Wietmarschen *et al.*, and the binding region was mapped. In our experiments, there was no interaction between MMS19 and CIAO1 (Fig. 4, *C* and *D*). On the basis of our data, we propose that MIP18 has a role to connect MMS19 and CIAO1. So far, the reasons causing the differences are unclear. One possible difference is the status of protein folding. We used recombinant proteins produced by insect cells to study protein-protein interactions. It is not clear whether *in vitro* translated proteins are properly folded or Fe-S clusters are sorted into the target site.

Collectively, possible models are proposed based on our *in vivo* and *in vitro* data. In both models, MMS19, MIP18, and CIAO1 form a tight core complex. The core complex catches and holds IOP1 via interaction with CIAO1. MMS19 in the complex binds apoproteins. MIP18 connects CIAO1 and MMS19. One model could be that the core complex plays roles

in the maturation of IOP1 (Fig. 5*A*). As IOP1 functions in the CIA pathway (36, 37) and it is a putative Fe-S cluster donor, Fe-S clusters might be further transferred from IOP1 to the target proteins by the full complex. However, studies in yeast show that Nar1 has already been matured in the early phase of the CIA pathway. In addition, it is not clear whether the core complex possesses Fe-S clusters or not. An alternative model is that, in human cells, the core complex may immediately catch and hold IOP1 when it is matured in the early phase of the CIA pathway. The core complex stabilizes IOP1 or prevents IOP1 from degradation. Then, the combined complex (full complex) may catalyze the late CIA reactions (Fig. 5*B*).

REFERENCES

1. Prakash, L., and Prakash, S. (1977) Isolation and characterization of MMS-sensitive mutants of *Saccharomyces cerevisiae*. *Genetics* **86,** 33–55
2. Askree, S. H., Yehuda, T., Smolikov, S., Gurevich, R., Hawk, J., Coker, C., Krauskopf, A., Kupiec, M., and McEachern, M. J. (2004) A genome-wide screen for *Saccharomyces cerevisiae* deletion mutants that affect telomere length. *Proc. Natl. Acad. Sci. U.S.A.* **101,** 8658–8663
3. Lauder, S., Bankmann, M., Guzder, S. N., Sung, P., Prakash, L., and Prakash, S. (1996) Dual requirement for the yeast *MMS19* gene in DNA repair and RNA polymerase II transcription. *Mol. Cell. Biol.* **16,** 6783–6793
4. Lombaerts, M., Tijsterman, M., Verhage, R. A., and Brouwer, J. (1997) *Saccharomyces cerevisiae mms19* mutants are deficient in transcription-coupled and global nucleotide excision repair. *Nucleic Acids Res.* **25,** 3974–3979
5. Queimado, L., Rao, M., Schultz, R. A., Koonin, E. V., Aravind, L., Nardo, T., Stefanini, M., and Friedberg, E. C. (2001) Cloning the human and mouse *MMS19* genes and functional complementation of a yeast *mms19* deletion mutant. *Nucleic Acids Res.* **29,** 1884–1891
6. Seroz, T., Winkler, G. S., Auriol, J., Verhage, R. A., Vermeulen, W., Smit, B., Brouwer, J., Eker, A. P., Weeda, G., Egly, J. M., and Hoeijmakers, J. H. (2000) Cloning of a human homolog of the yeast nucleotide excision repair gene *MMS19* and interaction with transcription repair factor TFIIH via the XPB and XPD helicases. *Nucleic Acids Res.* **28,** 4506–4513
7. Araújo, S. J., Tirode, F., Coin, F., Pospiech, H., Syväoja, J. E., Stucki, M., Hübscher, U., Egly, J. M., and Wood, R. D. (2000) Nucleotide excision repair of DNA with recombinant human proteins: definition of the minimal set of factors, active forms of TFIIH, and modulation by CAK. *Genes Dev.* **14,** 349–359
8. Kou, H., Zhou, Y., Gorospe, R. M., and Wang, Z. (2008) Mms19 protein functions in nucleotide excision repair by sustaining an adequate cellular concentration of the TFIIH component Rad3. *Proc. Natl. Acad. Sci. U.S.A.* **105,** 15714–15719
9. Beinert, H., Holm, R. H., and Münck, E. (1997) Iron-sulfur clusters: nature's modular, multipurpose structures. *Science* **277,** 653–659
10. Johnson, D. C., Dean, D. R., Smith, A. D., and Johnson, M. K. (2005) Structure, function, and formation of biological iron-sulfur clusters. *Annu. Rev. Biochem.* **74,** 247–281
11. Porello, S. L., Cannon, M. J., and David, S. S. (1998) A substrate recognition role for the $[4Fe\text{-}4S]^{2+}$ cluster of the DNA repair glycosylase MutY. *Biochemistry* **37,** 6465–6475
12. Wu, Y., and Brosh, R. M., Jr. (2012) DNA helicase and helicase-nuclease enzymes with a conserved iron-sulfur cluster. *Nucleic Acids Res.* **40,** 4247–4260
13. Rudolf, J., Makrantoni, V., Ingledew, W. J., Stark, M. J., and White, M. F. (2006) The DNA repair helicases XPD and FancJ have essential iron-sulfur domains. *Mol. Cell* **23,** 801–808
14. Liu, H., Rudolf, J., Johnson, K. A., McMahon, S. A., Oke, M., Carter, L., McRobbie, A. M., Brown, S. E., Naismith, J. H., and White, M. F. (2008) Structure of the DNA repair helicase XPD. *Cell* **133,** 801–812
15. Fan, L., Fuss, J. O., Cheng, Q. J., Arvai, A. S., Hammel, M., Roberts, V. A., Cooper, P. K., and Tainer, J. A. (2008) XPD helicase structures and activities: insights into the cancer and aging phenotypes from XPD mutations. *Cell* **133,** 789–800
16. Wolski, S. C., Kuper, J., Hänzelmann, P., Truglio, J. J., Croteau, D. L., Van Houten, B., and Kisker, C. (2008) Crystal structure of the FeS cluster-containing nucleotide excision repair helicase XPD. *PLoS Biol.* **6,** e149
17. Ito, S., Tan, L. J., Andoh, D., Narita, T., Seki, M., Hirano, Y., Narita, K., Kuraoka, I., Hiraoka, Y., and Tanaka, K. (2010) MMXD, a TFIIH-independent XPD-MMS19 protein complex involved in chromosome segregation. *Mol. Cell* **39,** 632–640
18. Balk, J., Aguilar Netz, D. J., Tepper, K., Pierik, A. J., and Lill, R. (2005) The essential WD40 protein Cia1 is involved in a late step of cytosolic and nuclear iron-sulfur protein assembly. *Mol. Cell. Biol.* **25,** 10833–10841
19. Takedachi, A., Saijo, M., and Tanaka, K. (2010) DDB2 complex-mediated ubiquitylation around DNA damage is oppositely regulated by XPC and Ku and contributes to the recruitment of XPA. *Mol. Cell. Biol.* **30,** 2708–2723
20. de Winter, J. P., and Joenje, H. (2009) The genetic and molecular basis of Fanconi anemia. *Mutat. Res.* **668,** 11–19
21. Wu, Y., and Brosh, R. M., Jr. (2009) FANCJ helicase operates in the Fanconi Anemia DNA repair pathway and the response to replicational stress. *Curr. Mol. Med.* **9,** 470–482
22. Barber, L. J., Youds, J. L., Ward, J. D., McIlwraith, M. J., O'Neil, N. J., Petalcorin, M. I., Martin, J. S., Collis, S. J., Cantor, S. B., Auclair, M., Tissenbaum, H., West, S. C., Rose, A. M., and Boulton, S. J. (2008) RTEL1 maintains genomic stability by suppressing homologous recombination. *Cell* **135,** 261–271
23. Peng, M., Litman, R., Xie, J., Sharma, S., Brosh, R. M., Jr., and Cantor, S. B. (2007) The FANCJ/MutLα interaction is required for correction of the cross-link response in FA-J cells. *EMBO J.* **26,** 3238–3249
24. Urzica, E., Pierik, A. J., Mühlenhoff, U., and Lill, R. (2009) Crucial role of conserved cysteine residues in the assembly of two iron-sulfur clusters on the CIA protein Nar1. *Biochemistry* **48,** 4946–4958
25. Stehling, O., Netz, D. J., Niggemeyer, B., Rösser, R., Eisenstein, R. S., Puccio, H., Pierik, A. J., and Lill, R. (2008) Human Nbp35 is essential for both cytosolic iron-sulfur protein assembly and iron homeostasis. *Mol. Cell. Biol.* **28,** 5517–5528
26. Levitus, M., Waisfisz, Q., Godthelp, B. C., de Vries, Y., Hussain, S., Wiegant, W. W., Elghalbzouri-Maghrani, E., Steltenpool, J., Rooimans, M. A., Pals, G., Arwert, F., Mathew, C. G., Zdzienicka, M. Z., Hiom, K., De Winter, J. P., and Joenje, H. (2005) The DNA helicase BRIP1 is defective in Fanconi anemia complementation group J. *Nat. Genet.* **37,** 934–935
27. Levran, O., Attwooll, C., Henry, R. T., Milton, K. L., Neveling, K., Rio, P., Batish, S. D., Kalb, R., Velleuer, E., Barral, S., Ott, J., Petrini, J., Schindler, D., Hanenberg, H., and Auerbach, A. D. (2005) The BRCA1-interacting helicase BRIP1 is deficient in Fanconi anemia. *Nat. Genet.* **37,** 931–933
28. Litman, R., Peng, M., Jin, Z., Zhang, F., Zhang, J., Powell, S., Andreassen, P. R., and Cantor, S. B. (2005) BACH1 is critical for homologous recombination and appears to be the Fanconi anemia gene product FANCJ. *Cancer Cell* **8,** 255–265
29. Wang, Z., Svejstrup, J. Q., Feaver, W. J., Wu, X., Kornberg, R. D., and Friedberg, E. C. (1994) Transcription factor b (TFIIH) is required during nucleotide-excision repair in yeast. *Nature* **368,** 74–76
30. Parish, J. L., Rosa, J., Wang, X., Lahti, J. M., Doxsey, S. J., and Androphy, E. J. (2006) The DNA helicase ChlR1 is required for sister chromatid cohesion in mammalian cells. *J. Cell Sci.* **119,** 4857–4865
31. Netz, D. J., Stith, C. M., Stümpfig, M., Köpf, G., Vogel, D., Genau, H. M., Stodola, J. L., Lill, R., Burgers, P. M., and Pierik, A. J. (2012) Eukaryotic DNA polymerases require an iron-sulfur cluster for the formation of active complexes. *Nat. Chem. Biol.* **8,** 125–132
32. Sonoda, E., Okada, T., Zhao, G. Y., Tateishi, S., Araki, K., Yamaizumi, M., Yagi, T., Verkaik, N. S., van Gent, D. C., Takata, M., and Takeda, S. (2003) Multiple roles of Rev3, the catalytic subunit of polζ in maintaining genome stability in vertebrates. *EMBO J.* **22,** 3188–3197
33. Gari, K., León Ortiz, A. M., Borel, V., Flynn, H., Skehel, J. M., and Boulton, S. J. (2012) MMS19 links cytoplasmic iron-sulfur cluster assembly to DNA metabolism. *Science* **337,** 243–245
34. Stehling, O., Vashisht, A. A., Mascarenhas, J., Jonsson, Z. O., Sharma, T.,

Netz, D. J., Pierik, A. J., Wohlschlegel, J. A., and Lill, R. (2012) MMS19 assembles iron-sulfur proteins required for DNA metabolism and genomic integrity. *Science* **337,** 195–199
35. Andrade, M. A., and Bork, P. (1995) HEAT repeats in the Huntington's disease protein. *Nat. Genet.* **11,** 115–116
36. Song, D., and Lee, F. S. (2008) A role for IOP1 in mammalian cytosolic iron-sulfur protein biogenesis. *J. Biol. Chem.* **283,** 9231–9238
37. Song, D., and Lee, F. S. (2011) Mouse knock-out of IOP1 protein reveals its essential role in mammalian cytosolic iron-sulfur protein biogenesis. *J. Biol. Chem.* **286,** 15797–15805
38. van Wietmarschen, N., Moradian, A., Morin, G. B., Lansdorp, P. M., and Uringa, E. J.(2012) The mammalian proteins MMS19, MIP18, and ANT2 are involved in cytoplasmic iron-sulfur cluster protein assembly. *J. Biol. Chem.* **287,** 43351–43358